

# The potential of $\text{YBa}_2\text{Cu}_3\text{O}_{7-x}$ for catalytic oxidation reactions in a radio frequency reactor

A. OVENSTON\*, J. R. WALLS

*Department of Chemical Engineering, University of Bradford, West Yorkshire, BD7 1DP, UK*

A. ALLEN, W. ARMSTRONG

*School of Science and Technology, University of Teesside, Cleveland, TS1 3BA, UK*

A ceramic composite containing the high-temperature superconductor  $\text{YBa}_2\text{Cu}_3\text{O}_{7-x}$  and alumina has ideal characteristics for absorbing energy from radio-frequency (r.f.) electromagnetic fields at high temperatures. It is an effective catalyst for the oxidation of methane in a cyclic mode of operation in which methane and air are fed consecutively to the reactor. Lattice oxygen is alternatively consumed to form  $\text{CO}_x$  and water and then regenerated. This facile movement of oxygen anions was monitored by following the cyclic changes in electrical conductivity. In a conventional tubular reactor at 1000 K, the products are largely those of total oxidation. In contrast, preliminary work in an r.f. reactor showed evidence of some production of  $\text{C}_2\text{s}$  from the methane coupling reaction.

## 1. Introduction

The development of a reactor heated by radio-frequency (r.f.) power has led to the design of catalysts to simultaneously satisfy two demands [1]. First, the material must have sufficient magnetic and/or dielectric loss to absorb energy from the electromagnetic field and so to reach and maintain the reaction temperatures, but the possibility of thermal runaway occurring must be prevented [2]. Secondly, it must possess all the desired catalytic characteristics, that is, have an active, but selective, long life. These two criteria are to some extent compatible in that a high and stable alternating-current (a.c.) conductivity is required at reaction temperatures, and for many reactions involving hydrocarbons good mobility of charge carriers is required in the bulk of the material in order to supply specific charges (electrons and ions) to catalytic sites at the surface of the materials [3, 4].

Certain mixed-oxide materials of high conductivity have been found to be suitable for the steam reforming of heavy oils and residues, coupled with the production of more ethylene and propylene than conventional catalysts under the same conditions [5]. The main advantage of the electromagnetic method of heating is that heat is supplied directly to the catalyst and not to the surrounding fluids, thus gas-phase cracking reactions can be successfully avoided [6].

Much recent research activity has been associated with the difficult quest of obtaining higher hydrocarbons from methane, with or without co-fed oxygen [7, 8]. One of the problems is deactivation by fouling. The r.f. reactor is potentially suitable for such reactions, and with a new design incorporating a fluidized bed some of the inherent problems of conventional

reactors can be avoided [8, 9]. Complex oxides may be used to control the catalytic performance of solids. Thomas [10] suggests that a particularly useful property is the capacity for facile loss of structural oxygen, which is associated with the concentration of oxygen-anion vacancies. Solid oxides such as perovskites, defective fluorites and pyrochlores are potential candidates. Such materials should be suitable for the catalytic partial oxidation of methane to higher hydrocarbons [4]. The oxidation of CO to  $\text{CO}_2$  over some of the high-temperature superconducting materials has been investigated in some detail. Carberry *et al.* have shown that  $\text{La}_{1-x}\text{Sr}_x\text{CrO}_{3-\delta}$  and  $\text{La}_{2-x}\text{Sr}_x\text{CuO}_{4-\delta}$  compare favourably with supported platinum for this reaction [11, 12]. For the latter material, the maximum activity was found at  $x = 0.4$ , and the variation with  $x$  was coupled to variation of the conductivity, the lattice parameter, the oxygen-vacancy concentration and the thermodynamic activity of SrO. At reaction temperatures of 373 to 523 K these solids have a high electronic conductivity. This reaction has also been conducted over the high-temperature superconductor  $\text{YBa}_2\text{Cu}_3\text{O}_{7-x}$  (YBCO) [13]. Structural oxygen is removed sacrificially and the deficit is replenished by gaseous oxygen. Thermogravimetric analysis (TGA) showed the uptake of the oxygen to be smooth, reversible and rapid at temperatures as low as 673 K. Other work at lower temperatures between 433 and 473 K showed that oxygen-deficient samples were more active than oxygen-rich samples due to the higher concentration of oxygen surface vacancies and defects [14]. Others have found that the insulating material  $\text{Y}_2\text{BaCuO}_5$  has a high stable activity for CO oxidation when it is slightly

\* Author to whom correspondence should be addressed.

reduced [15]. Ammoxidation of toluene over various Y–Ba–Cu–Co–O perovskites has been performed at 673 K [16]. Rare-earth tin oxides of the pyrochlore type ( $\text{Ln}_2\text{SnO}_7$ ), have been reported to be good catalysts for the oxidative coupling of methane (OCM) to ethylene [17]. The partial oxidation of  $\text{CH}_4$  to a synthesis gas has been investigated over  $\text{Ln}_2\text{Ru}_2\text{O}_7$  catalysts at about 1050 K [18]. An induction period of 30 min was required, and negligible loss of activity and selectivity occurred over a week.

The electrochemical oxidative dimerization of  $\text{CH}_4$  in Solid Oxide Fuel Cells (SOFCs) using perovskite-anode electrocatalysts has also been considered [19–21]. Using 8 mol % Ytria-stabilized zirconia at 1073 to 1223 K,  $\text{C}_2$  yields of up to 11% were achieved, with selectivities to ethylene and ethane of up to 55% [21]. It was found that the electronic and concomitant catalytic properties could be altered dramatically and reversibly using SOFCs.

The general requirements for co-feed catalysts suitable for OCM seem to be basic, irreducible oxides which form stable carbonate species [22]. These are high-temperature p-type semiconductors under normal operating oxygen partial pressures. Correlations between conductivity and  $P_{\text{O}_2}$  should help resolve which active species are involved. High-temperature superconductors, which also may have a high a.c. conductivity under reaction conditions have potential for use as catalysts in electromagnetic fields, providing they remain both physically and chemically stable. Coupled with the unique feature of such reactor design to eliminate fouling reactions, and to control temperature effectively and rapidly, these materials may be suitable for this novel route for difficult reactions such as the partial oxidation of methane. A preliminary study is reported here. The a.c. electrical properties of composites containing  $\text{YBa}_2\text{Cu}_3\text{O}_{7-x}$  and alumina have been studied in inert, oxidizing and methane atmospheres up to 1000 K, between 100 Hz and 10 MHz. The heating characteristics in a small-scale r.f. reactor have been measured, and the catalytic potential of such material is illustrated, with a close correlation between the activity and conductivity being shown.

### 1.1. Properties of $\text{YBa}_2\text{Cu}_3\text{O}_{7-x}$ at elevated temperatures

YBCO is a mixed conductor above about 573 K. The variation of the electrical conductivity between room temperature and 1250 K (when it starts to decompose [23]) is highly complex. The conductivity of a polycrystalline sample is dependent on its history, that is, its method of preparation and the pre-sintering procedure, and the thermal cycling it may have undergone. The influence of the sintering temperature, the sintering and annealing atmospheres, and the quench rate on the properties of YBCO have been studied [24]. The phase responsible for superconductivity is  $\text{YBa}_2\text{Cu}_3\text{O}_{7-x}$ ,  $x < 0.5$ , having a distorted oxygen-deficient, perovskite-like, orthorhombic structure. Between 573 and 773 K in air, the oxygen anion

conductivity varies from  $10^{-3}$  to  $10^2 \text{ S m}^{-1}$ . Activated behaviour is shown with  $E_A$  between 2.5 and 2.6 eV above 663 K and equal to about 2.2 eV below 643 K [25]. The origin of the ionic conductivity is related to the electrical mobility and concentration of point defects. At 1073 K the chemical diffusion coefficients for oxygen in both  $\text{YBa}_2\text{Cu}_3\text{O}_{7-x}$  and  $\text{La}_{0.5}\text{Sr}_{0.5}\text{MnO}_{3-y}$  (another mixed-conductor perovskite bronze material) have been found to be significantly larger than those measured for oxide-ion conductors at comparable temperatures [26]. Defect models have been proposed for both YBCO and an La–Sr–Cu–O system [27]. Redox reactions at high temperatures can lead to large variations in the free-carrier density. Furthermore, the contribution of electronic conductivity cannot be ignored, this generally increases as  $P_{\text{O}_2}$  increases.

Nowotny *et al.* and Molenda *et al.* have reviewed and studied the defect structures and transport properties of YBCO at elevated temperatures in detail [23, 28–30]. A  $T$ – $P_{\text{O}_2}$  phase diagram showing different conducting regions has been constructed [23]. A quasi-metallic-to-semiconducting transition occurs at 950 K for  $P_{\text{O}_2} = 10^2 \text{ Pa}$  and alters to  $10^4 \text{ Pa}$  at 1150 K; p–n transitions have been observed in the semiconducting region. Transitions between tetragonal and orthorhombic structural phases also occur. At 950 K, YBCO is likely to be tetragonal; whilst below 900 K, a tetragonal to orthorhombic transition is likely. Up to 1000 K, the material should be quasi-metallic. The electrical conductivity decreases with increasing temperature, but the behaviour is not metallic since the concentration of ions and electronic defects is connected with  $x$ , which itself increases with increasing temperature [29–30]. At about 650 K,  $x \leq 0.1$  and the structure is orthorhombic, but at temperatures closer to 950 K,  $x$  could vary between 0.2 and 0.6 with an orthorhombic-to-tetragonal phase transition between  $x = 0.3$  and 0.4. At any given temperature, increasing  $x$  is accompanied by a decreasing conductivity [30]. For the orthorhombic phase and values of  $x < 0.3$  at 650 to 800 K, semiconducting behaviour was observed with  $E_A \approx 0.2 \text{ eV}$ . Typically, at 1000 K in air, at ambient pressure, quoted values for the conductivity vary between  $5 \times 10^2$  and  $2 \times 10^4 \text{ S m}^{-1}$ ; at 700 K it is about  $2 \times 10^3$  to  $2 \times 10^4 \text{ S m}^{-1}$  [23, 29–31]. Nowotny and Rekas found that a simple hopping model could not be fitted to the measured data; a better model was fitted in which interaction between both electrons and holes was taken into account as well as interactions between defects, arising from their very high concentrations [29]. A model for the defect structure is also given by Molenda *et al.* [30] and it has been fully confirmed by electrical measurements obtained under conditions of thermodynamic equilibrium.

At room temperature, the conductivity depends on the sintering prehistory, and changes from the tetragonal to the orthorhombic phase have been observed after repeated cycles of 6 h sintering at 950 K [32]. Thus the conductivity can vary between semiconducting behaviour with conductivities of the order of  $2 \times 10^3 \text{ S m}^{-1}$  to metallic behaviour with values of

about  $5 \times 10^5 \text{ S m}^{-1}$ . An increase in  $x$  induces the orthogonal-to-tetragonal transitions, and the material may become non-superconducting at very low temperatures. The heat capacities of  $\text{YBa}_2\text{Cu}_3\text{O}_{7-x}$  ( $x = 0, 0.18, 0.35$  and  $0.6$ ) have been measured between room temperature and 800 K [33]. An anomaly was observed above 700 K for  $x = 0.35$ , and it correlated with the phase transition from the orthorhombic-I to the orthorhombic-II structure. No anomalies were observed for  $x = 0.18$  (orthorhombic-I) or  $x = 0.6$  (tetragonal). YBCO is known to show metastable behaviour with regard to water,  $\text{CO}_2$  and other solvents [34]. The thermal stability has been studied over the temperature range 573 to 1223 K for a  $P_{\text{O}_2}$  of 4 Pa to 1 atmosphere and a  $P_{\text{CO}_2}$  of  $10^{-4}$  Pa to 1 atmosphere. A stability field of the orthorhombic and tetragonal phases showed a region of coexistence dependent on the oxygen partial pressure. The properties of YBCO are particularly dependent on the many processing parameters involved in the manufacturing process; for example, the decomposition of the superconducting phase is strongly influenced by a small amount of  $\text{CO}_2$  (1 p.p.m. (part per million)) in the sintering atmosphere.

Melt-quenched YBCO is known to react strongly with  $\text{Al}_2\text{O}_3$ ,  $\text{ZrO}_2$  and  $\text{SiO}_2$ , and new phases (for example,  $\text{BaAl}_2\text{O}_4$ ,  $\text{BaZrO}_3$  and  $\text{Ba}_2\text{SiO}_4$ ) can be formed [35]. Hence reactions may also occur when YBCO powder is pelleted with  $\text{Al}_2\text{O}_3$  and the composite is subjected to high temperatures in an r.f. heater. Such solid-state reactions can be monitored by a.c. electrical studies, since any changes undergone are reflected in changes in the conductivity with time; this will be the subject of further experiments.

## 2. Experimental methods

### 2.1. Preparation of material

The  $\text{YBa}_2\text{Cu}_3\text{O}_{7-x}$  powders were synthesized by the solid-state reaction method from  $\text{Y}_2\text{O}_3$  (99.99% pure),  $\text{BaCO}_3$  (99.999% pure) and  $\text{CuO}$  (99.999% pure) in stoichiometric proportions. The oxides were crushed, mixed and pelleted, heated at  $25 \text{ K min}^{-1}$  up to 1073 K, held at this temperature for 10 min, further heated at  $10 \text{ K min}^{-1}$  up to 1313 K and then sintered at this temperature for 12 h, and finally cooled at  $1 \text{ K min}^{-1}$ . The powder was recrushed and compressed into pellets 10 mm diameter and about 5 mm long. The sintering process was then repeated. Small pieces of the material were cooled to liquid-nitrogen temperatures and suspended in a magnetic field; the expulsion from the field (the Meissner effect) demonstrated the superconductivity of the material.

For composite pellets, after the first sintering, the crushed powder was mixed with 50 wt %  $\gamma\text{-Al}_2\text{O}_3$  pelleted and resintered. Pellets 1 cm in diameter, 0.7 cm in length, and also larger pellets 1.5 cm in diameter and 1 cm in length, were also made. For the samples required for electrical studies, platinum contacts were made by firing on platinum-based enamel (Johnson Matthey E-831) at 1000 K for 1 h. TGA studies of the composite showed instability above about 1150 K.

### 2.2. Heating curves

Several large pellets were placed in the reactor tube (Fig. 1) on glass raschig rings. The tube was positioned so that the pellets were surrounded by the r.f. coil. The reactor tube was purged with an inert gas before the power was applied. Initially argon was used; but, due to the production of a plasma inside the tube when the power was applied, nitrogen was used in subsequent experiments. The voltage was slowly increased from zero to 6.75 kV, and the temperature was recorded as a function of time using a fibre-optics probe directed at the centre of the reactor tube. On reaching an equilibrium temperature, the voltage was held constant for several minutes before slowly being reduced to zero.

### 2.3. Electrical measurements

Single pellets with platinum contacts were held under compression in a programmable, gold, reflecting tubular furnace (Eurotherm 106 + unit 812) through which gases could be passed at constant rates, controlled by Brookes flowmeters. Low loss, high temperature, British Insulation Cable Co. (BICC) cable was used for the connections inside the furnace, which were connected to Hewlett Packard leads outside the furnace and to a Hewlett-Packard gain-phase/impedance analyser 4194A. For the conductivity measurements, the sample was represented by a resistance in parallel with

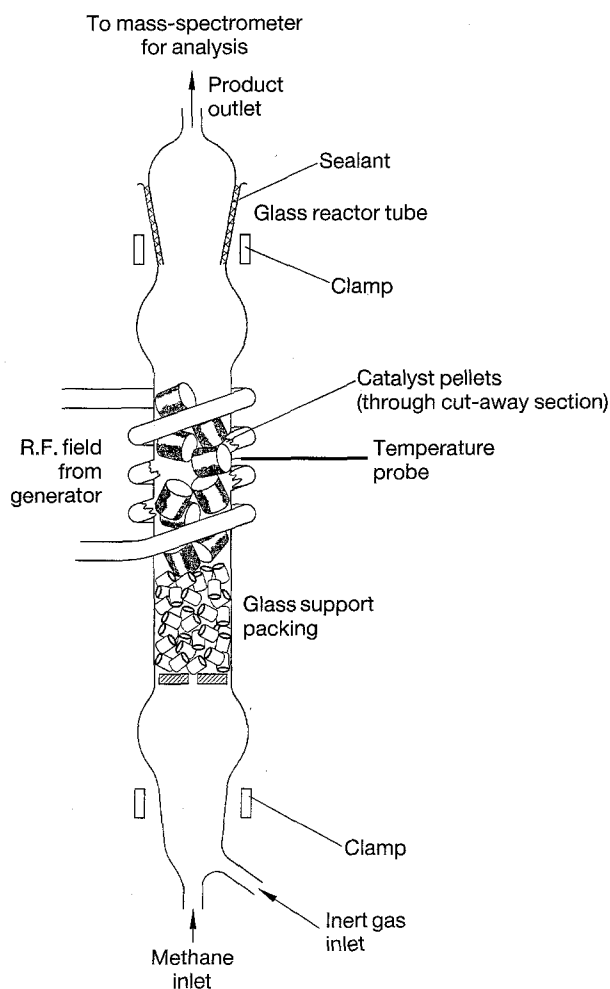


Figure 1 The 20 MHz r.f. reactor.

a capacitance, whilst for complex impedance diagrams, the sample was represented by a resistance in series with a capacitance, as described in more detail in [36]. For the former, measurements were made at 21 frequencies between 100 Hz and 10 MHz, whilst for the latter 401 frequency points were measured between 100 Hz and 2.5 MHz. To study the effect of the gaseous atmosphere, measurements were automatically recorded at 5 min intervals.

## 2.4. Product distribution

Exit gases from the reactor tubes, after passing over a moisture trap, were analysed by a VG quadrupole mass spectrometer. For coupling with the measurements of the conductivity, the products were analysed simultaneously with the electrical measurements, using a single pellet with a platinum contact. For larger effects to be observed, the reactor tube was packed with 15 of the larger-sized pellets and the quantity of products was correspondingly magnified. For comparison with various hydrocarbons, samples of pure ethylene, ethane, propylene and propane were analysed. Since at r.f. argon causes a plasma at radio frequencies and nitrogen has the same molecular weight as CO and C<sub>2</sub>H<sub>4</sub>, helium was used as a carrier gas for the methane.

## 3. Results

### 3.1. A.C. conductivity

Conductance measurements for single pellets of YBCO alone and for the YBCO/Al<sub>2</sub>O<sub>3</sub> composite, for the temperature range 300 to 950 K, in an argon atmosphere, are shown in Fig. 2. For YBCO the effect of the frequency was negligible, and behaviour typical of a low-band gap semiconductor was observed with a low activation energy of the order of 0.1 eV. For the composite pellet, the conductance was reduced by about three orders of magnitude and it showed a slight dependence on frequency. A value for the effective conductivity is given by  $Gd^2/4l$ , where  $G$  is the conductance, and  $d$  and  $l$  are the diameter and length of

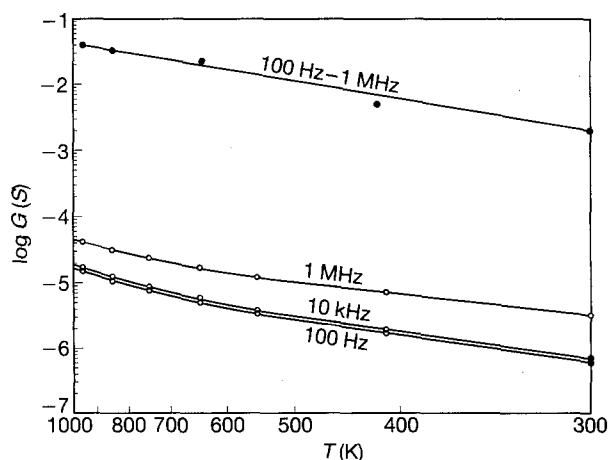


Figure 2 The conductance of (●) the YBCO pellet alone and (○) the YBCO/alumina composite in Ar as a function of the frequency and the reciprocal temperature.

the pellet, respectively. Values for the conductivity extrapolated to a frequency of 20 MHz, the r.f. reactor frequency, are shown in Fig. 3. These may be compared with the frequency-temperature characteristic for a catalyst composite containing K<sub>0.5</sub>WO<sub>3</sub> and cement examined previously [2]. This material containing the mixed conductor, an alkali tungsten bronze, had been proved to heat rapidly and to maintain the reaction temperatures up to 1000 K at 20 MHz [1].

For the superconducting material, the effect of the frequency was low at all temperatures. For example, at 550 K, the dependence was  $\sigma \propto \omega^{0.12}$ , whilst at 950 K it was  $\sigma \propto \omega^{0.014}$  between 1 kHz and 1 MHz. Complex impedance measurements were made for a larger sample of the composite material with  $d = 1.5$  cm and  $l = 1$  cm. For this material, the effect of the frequency was greater with  $\sigma \propto \omega^{0.33}$  and  $\sigma \propto \omega^{0.25}$  at 550 and 950 K, respectively. Complex impedance diagrams for temperatures between 450 and 950 K (Fig. 4) showed no low-frequency spurs, as have been observed for other composites containing mobile ions [36]; tilted semicircular plots, with angles of tilt to the real axis of about 20° and a flattening of the arc at the high frequencies, are seen, with no evidence for separate arcs or semicircles for grain boundary and bulk effects, as is often found for polycrystalline ionic conductors [37].

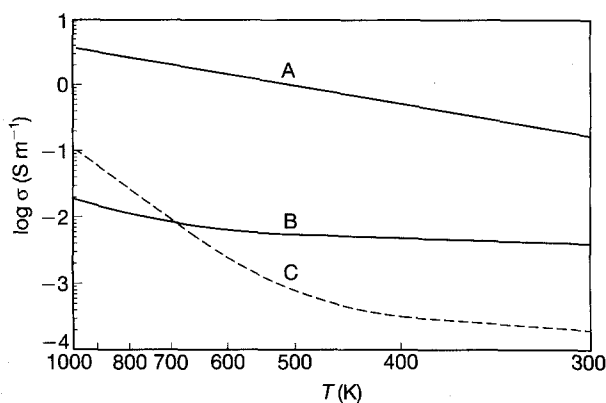


Figure 3 The conductivities at 20 MHz (extrapolated) as a function of the reciprocal temperature for: (A) YBCO, (B) YBCO/alumina composite (50:50 wt %), and (C) K<sub>0.5</sub>WO<sub>3</sub>/cement/alumina composite.

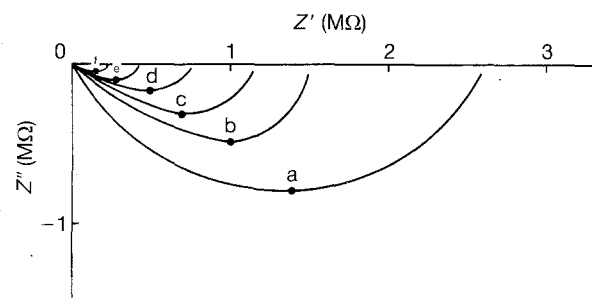


Figure 4 Complex impedance diagrams for the YBCO/alumina composite in Ar at (a) 450 K, (b) 550 K, (c) 650 K, (d) 750 K, (e) 850 K and (f) 950 K.

The critical frequencies at which  $Z''$  is in a minimum showed only a slight dependence on temperature between 450 and 650 K, but a more significant increase with temperatures above about 800 K. This change indicates that a change in the dielectric loss mechanism occurred around this temperature, possibly due to the increased mobility of oxygen anions and their contribution to dipole relaxation processes.

### 3.2. Heating and cooling at 20 MHz

Several pellets of YBCO placed in the reactor tube were found to heat up extremely rapidly at r.f.; thermal runaway also occurred, and the instrument had to be switched off after 4 kV had been reached. The pellets were found to have fused together and also to have fused to the vitreous silica tube, causing the latter to break. The conductivity of this material was clearly too high, hence further experiments were performed with a composite whose conductivity had been reduced by the addition of 50 wt % alumina. The heating and cooling characteristics for several large pellets of this material in a nitrogen atmosphere are shown in Fig. 5. For this material, any desired working temperature up to 1000 K could be achieved rapidly and maintained by altering the power input. Problems of thermal runaway did not occur.

Control of the conductivity between the ambient and the working temperature is important, since the energy absorbed in a given field is proportional to the a.c. conductivity, which is itself a function of temperature. Hence the final temperature achieved is dependent on heat losses due to convection and radiation [2]. If the low-temperature values for the conductivity are too low, the rate of heating may be too slow and working temperatures may never be achieved. If, on the other hand, the conductivity is too high at higher temperatures, then thermal runaway can occur. The optimum conductivity temperature characteristic is flat or with a slight decrease in the conductivity above the working temperature. Hence the properties of the YBCO composite were close to ideal, and reproducible heating curves were obtained for various settings of the input power.

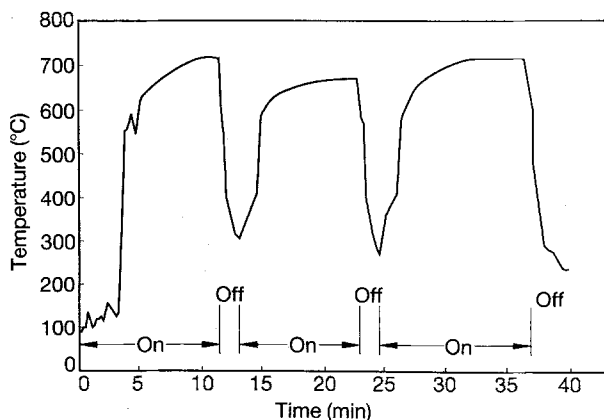


Figure 5 Heating and cooling curves for composite YBCO/alumina pellets in the 20 MHz reactor in Ar.

### 3.3. Effect of atmosphere on conductance

Preliminary experiments showed that the effect of hydrogen on the YBCO alone at 750 K was to cause a rapid rise in the conductance, followed by a slower reduction of the copper-oxide component to copper. This material exhibited semi-metallic behaviour and would thus be unsuitable for strongly reducing reactions at high temperatures. Detailed measurements of the effect of methane on the composite with alumina were made at 950 K. As shown in Fig. 6, the effect of methane diluted with argon, was a rapid reduction of the conductance at all frequencies, the lower the frequency the larger was the effect. On removal of the methane the conductance stabilized, and values close to the initial data could be achieved by re-oxidation of the material in air. These changes in conductance could be reproduced on repetition of the gas sequences. At 1 MHz, the conductance decreased by a factor of 8.5 after about 30 min in methane; at 1 kHz it decreased by a factor of 260. Whilst at lower frequencies the effects were greater but erratic.

### 3.4. Gaseous products from methane oxidation

#### 3.4.1. Tubular reactor

The tube was packed with 15 large pellets of the composite YBCO/ $\text{Al}_2\text{O}_3$  pellets, without platinum contacts, and a methane argon mixture ( $25:50 \text{ ml min}^{-1}$ ) was passed over the tube at 950 K. The product gas stream was analysed by the mass spectrometer. For material in a freshly oxidized state, products of CO and  $\text{CO}_2$  were observed, as shown in Fig. 7. Since the

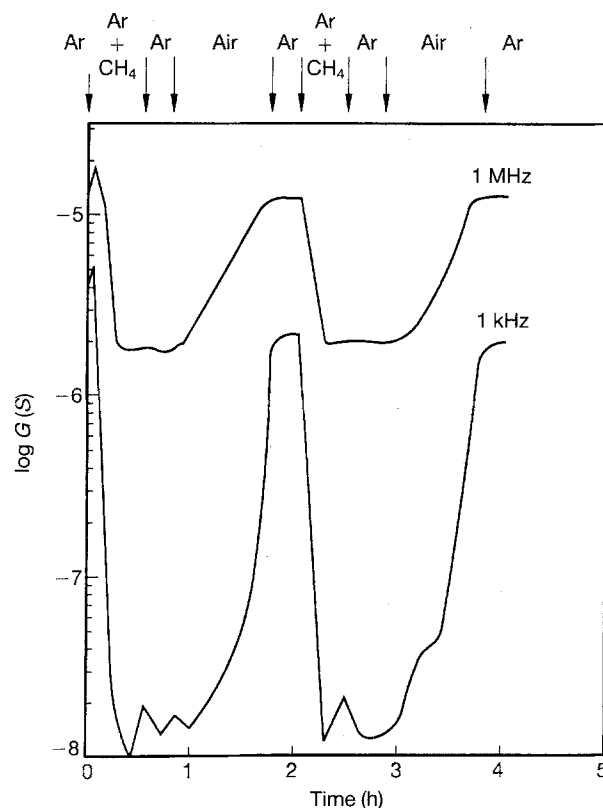


Figure 6 The effect of air and methane atmospheres on the conductance of YBCO/alumina pellets at 950 K at 1 kHz and 1 MHz.

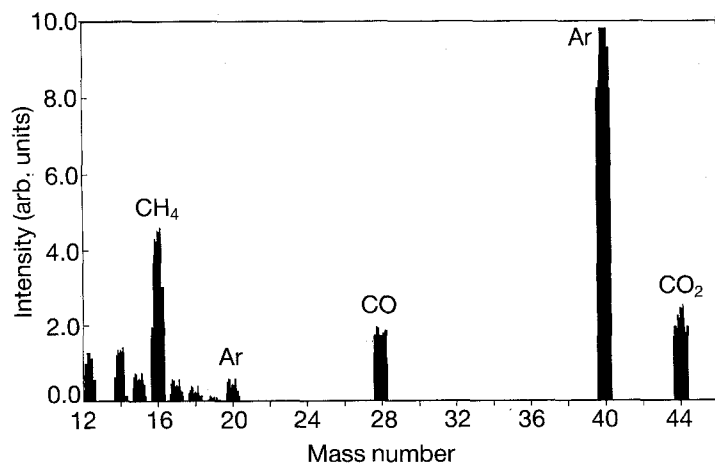


Figure 7 Mass spectrogram for complete combustion of methane in air at 950 K in a conventional tubular reactor.

reactant stream contained no oxygen, the oxygen must have come from lattice oxygen in the YBCO. With time, the amount of  $\text{CO}_2$  diminished and the amount of CO decreased more slowly until after about 90 min no further reaction occurred, as shown in Fig. 8a. This effect was consistent with the observation that the conductance decreased to a stable level in the presence of methane (Fig. 6). On re-oxidation in air, and subsequent removal of any gaseous oxygen by purging in argon, the cycle was reproduced with CO and  $\text{CO}_2$  being produced until all available oxygen had been used up. After about four cycles, the behaviour became reproducible (Fig. 8b). After re-oxidation

in air at 950 K for 2 h, an initially higher conversion of methane was achieved which favoured the production of  $\text{CO}_2$ ; this was followed by deactivation of the catalyst over about 30 min as the available oxygen became depleted.

In the absence of a catalyst, no products were obtained when a methane-air mixture was passed through the reactor tube at 950 K, illustrating the need for YBCO to catalyse the complete oxidation of methane at this temperature. The correlation with changes in the conductance was confirmed by repeating the reaction for a single pellet with platinum contacts, with measurements of conductance being made simultaneously with regular 5 minute sampling of the reaction products. The low-surface-area platinum did not appear to have a significant effect.

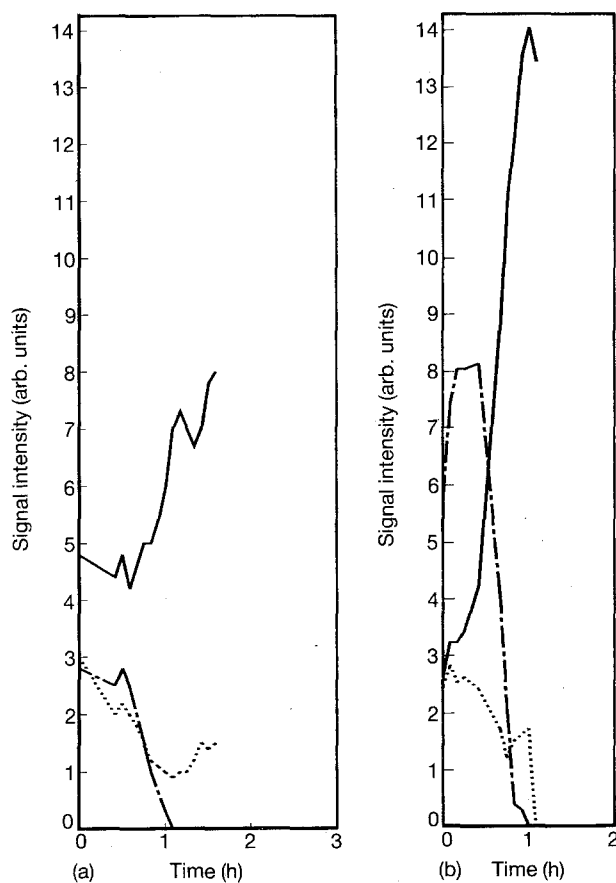


Figure 8 Time variation of signal intensities at mass numbers 16, 28 and 44 representing (—)  $\text{CH}_4$ , (.....) CO and (- - -)  $\text{CO}_2$  for methane oxidation at 950 K. (a) first cycle; (b) fifth cycle.

### 3.4.2. R.f. reactor

Methane and helium ( $5:25 \text{ ml min}^{-1}$ ) were passed over a bed of the composite catalyst (equivalent to about two large pellets) in the 20 MHz reactor operating at about 950 K. The product gases were found to contain mainly CO, with a small amount of species at mass numbers 44 ( $\text{CO}_2$ ), 26 and 30 in addition to mass number 28 (CO). Since methane alone gives no contributions at mass numbers 26 and 30, it is reasonable to assume that these contributions arise from the presence of traces of ethane and possibly some ethylene in the product distribution. Histograms for the intensities of mass numbers for pure ethane and pure ethylene show that ethane produces a signal at mass number 30, whilst the highest mass number recorded for pure ethylene is at mass number 28. Pure propane and propylene would produce signals at mass numbers between 36 and 44. Since no signals were observed in this region, apart from  $\text{CO}_2$  at mass number 44, it can be assumed that these higher hydrocarbons were not produced. Hence these results indicate that the methane is not completely oxidized in the electromagnetic reactor and activation of the catalyst by r.f. power may provide a novel route to the catalytic partial oxidation. These are preliminary experiments, using small quantities of catalyst in a small-scale r.f. reactor. Further work is underway to measure conversion rates and selectivities in a larger-scale fluidized bed r.f. reactor.

## 4. Discussion

### 4.1. High-temperature conductivity of YBCO

In the absence of platinum electrodes, the sample of YBCO placed between brass plates behaved like a semiconductor of low band gap with  $E_A \approx 0.1$  eV, with no significant effect due to the frequency. The conductivities were  $0.18$  and  $3.6 \text{ S m}^{-1}$  at  $300$  and  $950$  K, respectively. These values are considerably lower than those reported elsewhere; for semi-metallic behaviour the conductivity would be expected to be about  $2.5 \times 10^3$  at  $500$  K and  $4 \times 10^2$  at  $1000$  K [23]. It is possible that the comparatively low values observed arise from a relatively high porosity and/or not all the material being in the superconducting phase. With electrodes fired on in air at  $1000$  K for  $1$  h, the values at the highest frequencies were similar, but the conductance fell with reducing frequency. Since the application of the platinum introduced some additional thermal treatment, some variation in the behaviour is to be expected since YBCO is known to be particularly susceptible to its pre-history. Heating-cooling cycles between  $573$  and  $773$  K have been reported to have no effect on the values of the conductivity, but repeated cycles between ambient temperature and the higher temperature of  $973$  K were found to result in a systematic decrease in the ionic conductivity [25].

With electrodes present, the sample behaved like a lossy capacitance, with  $C_p$  the parallel capacitance virtually independent of the frequency and  $G$  only slightly dependent on the frequency, with, for example,  $G \propto \omega^{0.1}$  at  $550$  K. Complex impedance plots showed a well-defined semicircle with an angle of tilt to the real axis of less than  $10^\circ$ . No low-frequency spurs were obtained up to  $773$  K. Thus, at temperatures below  $773$  K, insignificant transport of ions is apparent [36]. In a nitrogen atmosphere, the conductivity of YBCO has been shown to have a semiconductor-like behaviour with an activation energy of about  $0.07$  eV below  $600$  K, with conductivities of order  $2 \times 10^2 \text{ S m}^{-1}$  at  $300$  K and  $7.5 \times 10^2 \text{ S m}^{-1}$  at  $950$  K [31]. These values are comparable to those recorded by Carrillo-Cabrera *et al.* [25] at high temperatures, although the latter exhibited quasi-metallic rather than semi-conducting characteristics, with the conductivity decreasing rather than increasing with increasing temperature. In oxygen, the degree of departure from stoichiometry is known to change with rising temperature. The extent of oxygen deficiency, decreases with increasing temperature, so that  $\text{YBa}_2\text{Cu}_3\text{O}_{7-x}$  becomes closer to the stoichiometric value at high temperatures; phase changes are often observed at about  $673$  K [31]. It is possible that  $x$  becomes quenched when the conductivity is measured in an inert atmosphere such as argon, and that as the temperature is increased  $x$  remains at a low value, and semi-conducting behaviour is observed and little ionic conductivity arising from oxygen anions is detected. Hence care should be taken when attempting to correlate values for the conductivity which have been measured in air or oxygen. The partial pressure of oxygen has a significant effect on the conductivity, with the conductivity increasing as  $P_{\text{O}_2}$  increases. Thus the ob-

served decrease in the conductance in methane, and the subsequent revival in air at high temperatures, is to be expected.

For the composite containing  $50$  wt % alumina, the characteristics showed a much increased effect of frequency due to the insulating properties of alumina, which would itself exhibit a strong dependence on frequency at all temperatures. By varying the proportions of the conductor to the insulator and the porosity of the composite it should be possible to obtain an effective conductivity varying between quasi-metallic, semi-conducting and insulating behaviour.

### 4.2. Heating curves

Using a simple model for the determination of heating and cooling curves in the  $20$  MHz reactor, and assuming that losses due to conduction are negligible, and that there is a negligible heat of reaction, then the energy absorbed from the electromagnetic field is offset by the energy lost by radiation and convection [2]. For this reactor containing two large pellets, at temperatures approaching  $1000$  K, the energy lost by radiation is about twice that lost by convection. From the energy-balance equation it can be shown that

$$\frac{dT}{dt} = \frac{[C_3 I^2 \omega^2 \sigma - C_1(T^4 - T_0^4) - C_2(T - T_0)^{1.25}]}{M(a + bT + cT^{-2})}$$

where  $a$ ,  $b$  and  $c$  are specific heat coefficients,  $M$  is the mass of the pellet, and  $I$  is the current in the r.f. coil. Assuming that the heat-transfer coefficients, specific-heat expressions and emissivity have the same values as those used in the models for other conductor-insulator composites, for a working temperature of  $1000$  K, values for  $C_1$ ,  $C_2$  and  $C_3$  are  $4.7 \times 10^{-11}$ ,  $6.4 \times 10^{-3}$  and  $2.34 \times 10^{-19}$  (SI units), respectively. At equilibrium  $dT/dt$  is zero, and an approximate value for the conductivity at  $20$  MHz can be determined. This value is estimated to be about  $2.8 \times 10^{-3} \text{ S m}^{-1}$  for a typical coil current at  $2.6$  kA, which is very close to the value of about  $2.6 \times 10^{-3} \text{ S m}^{-1}$  measured for a large pellet of the YBCO composite. Accurate assessment of the coil current and its relationship to the input power of the instrument would be required to confirm the accuracy of the model together with accurate heating and cooling-rate data.

At  $20$  MHz, the variations in conductivity with gaseous atmosphere are not likely to result in thermal instability of the reactor, which is controlled by a feedback loop linking the measured temperature with the input power. If a reactor of much lower frequency were used, the effect of the atmosphere on the conductivity would be enhanced, and the possible problem of instability would need investigation.

### 4.3. $\text{YBa}_2\text{Cu}_3\text{O}_{7-x}$ for catalytic use in an r.f. reactor

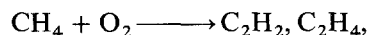
The potential of the r.f. route to control fouling problems in the steam reforming of heavy hydrocarbons has already been proved [6]. Its application to oxidation reactions has yet to be explored. Poirier *et al.* in a comprehensive review of the catalytic conversion of

methane concluded that new process configurations are required to obtain an economically viable process [8]. Short reaction times may be necessary to avoid carbon formation, and better control of the large exotherm associated with OCM is anticipated with fluidized beds rather than the conventional fixed-bed operation. For OCM on NaOH/CaO or pure CaO catalysts, the application of the fluidized bed reactor has already been demonstrated to be more favourable than a packed-fluidized-bed reactor with regard to operability and  $C_{2+}$  selectivity [38]. Commonwealth Scientific Industrial Research Organization (CSIRO) report that methane coupling and pyrolysis of higher alkanes can be effectively combined with a single fluidized-bed reactor, forming the Oxidative Coupling (OXCO) process for the total utilization of natural gas in Australia [39]. Arco Chemical Co., USA, advocate a thin-bed reactor placed in a heat-conductive catalyst holder. An incoming gas feed cools the catalyst holder and bed and so prevents excessively high temperatures [40]. Dautzenberg *et al.* (Catalytica Inc) and Rostrup-Nielsen (Haldor-Topsoe) have also assessed the multi-tubular reactor and the fluidized-bed reactor for their cost effectiveness for OCM [41]. They concluded that the latter could be technically feasible, with its key advantage of uniformity of temperature within the catalyst bed, offering control of selectivity without problems of hot spots. In addition cold feeds can be introduced with fluidized beds, and a large proportion of the heat of reaction can therefore be absorbed as sensible heat.

Since YBCO decomposes in air at 1250 K, it is vital that overheating should be avoided. Cooling is also important; if the material is quenched at about 800 K, phase changes may occur resulting in changes in both electrical and catalytic properties. With the use of electromagnetic power to heat the catalyst, temperatures can be controlled much more readily and rapidly than in conventional reactors. Preliminary tests using a larger-scale, fluidized-bed r.f. reactor have been encouraging. Hence this technique shows promise for many reactions for which control of the catalyst temperature is desirable without overheating of the ambient atmosphere; thereby undesirable side reactions may be controlled or even eliminated. With this method it would be relatively easy to control the exothermicity of OCM reactions by cooling the fluidized bed with an incoming flow of cold reactant gases.

This paper has illustrated that the electrical properties of YBCO can be controlled with the addition of an insulator to give almost ideal characteristics at radio frequencies, that is, a high a.c. conductivity which is almost independent of temperature and hence will not result in problems of thermal runaway. Such a material, with its unique oxygen-anion behaviour, where lattice oxygen can be easily removed or replaced, is thought to be particularly suited to the oxidative coupling reactions [4]. Catalysts operate in the co-feed mode or in the cyclic mode; that is, methane and oxygen are alternatively passed over the catalyst. Catalysts which operate in the cyclic mode must have an oxygen-storage capacity, a feature of the high-temperature superconductors.

Lunsford has discussed the possible mechanism for the conversion of methane to higher hydrocarbons over a variety of materials [42, 43], that is,



higher hydrocarbons,  $\text{H}_2\text{O}$ ,  $\text{CO}$ ,  $\text{CO}_2$ ,  $\text{H}_2$

Using metal-oxide catalysts, OCM is now generally considered to be a heterogeneous-homogeneous reaction in which surface-generated  $\text{CH}_3\cdot$  radicals initiate a gas-phase reaction. These chain-branching reactions consume additional methane and are partly responsible for the conversion of  $\text{CH}_4$  to  $\text{C}_2\text{H}_2$  and  $\text{C}_2\text{H}_4$  and for the formation of  $\text{CO}_x$ . Secondary reactions of  $\text{CH}_3\cdot$  radicals with the metal oxide may also contribute to the formation of  $\text{CO}_x$  [43]. Factors such as the  $\text{CH}_4:\text{O}_2$  ratio, the total pressure of the reactants, the  $\text{CH}_4$  conversion rate, the temperature, the free volume of the reactor and the type of catalyst all play a role in determining the major source of  $\text{CO}_x$ . Basic oxides promoted with alkali-metal carbonates form an important class of oxidation dimerization catalysts. Lithium or sodium ions may play several roles depending on the temperature [42]. Relationships between the conductivity and the oxygen partial pressure could help resolve the nature of the active species involved [22].

Consistency of the material is particularly important for any type of reactor; the properties of YBCO are known to be sensitive to its method of preparation and to its pre-history; for example, the temperature of sintering is extremely important for adjusting the initial values of the non-stoichiometry in the metal sublattice [25]. The presence of water has been found to reversibly reduce the activity of YBCO for the oxidation of CO, probably as a result of competitive adsorption with CO [14]. When water was mixed with YBCO and a cement and allowed to set, the resulting composite had a conductivity considerably lower than that obtained with a pelleted mixture of YBCO and alumina. YBCO has also been used as a catalyst for the decomposition of NO, but sintering problems arose at temperatures above 1073 K [44]. The addition of MgO suppressed this problem.

Many transition-metal perovskites are known to react with stable oxides such as  $\text{Al}_2\text{O}_3$ ,  $\text{ZrO}_2$ . Yokokawa *et al.* have studied the possible interface reactions between electrode and electrolyte materials in solid-oxide fuel cells (for example, in [45]); their methods of thermodynamic analysis using chemical-potential diagrams [46] could be applied to possible interface problems between YBCO and  $\text{Al}_2\text{O}_3$ , should this pose a significant problem. Melt-quenched YBCO has been reported to react with  $\text{Al}_2\text{O}_3$ ,  $\text{ZrO}_2$  and  $\text{SiO}_2$  with new phases, for example,  $\text{BaAl}_2\text{O}_4$ ,  $\text{BaZrO}_3$  and  $\text{Ba}_2\text{SiO}_4$ , being formed [35]. Such solid-state reactions can be monitored by a.c. techniques, since any changes in the chemical or physical state are reflected in changes in conductivity with time, coupled with X-ray diffraction (XRD) studies. Changes in electrical properties in an inert atmosphere are unlikely to be distorted by sintering [47] since YBCO has already been sintered during preparation. Should any interfacial



reactions seriously reduce the efficacy of the material, then other ceramic oxides could be considered as an alternative to alumina. D.c. electrical conductivity methods have been used for studying non-steady-state conditions to follow the response of reactants and products to methane coupling on ZnO-based catalysts [48]. Jiang *et al.* [49], using the four-probe d.c. method, have studied the effect of  $x$  on the catalytic oxidation of CO over YBCO and they showed that the catalyst itself could supply sufficient oxygen from the lattice. Generally, the lower the value of  $x$  ( $< 0.9$ ) the higher and more "metallic" is the conductivity and the greater is the activity. The oxygen is supplied by the surface lattice oxygen and the oxygen vacancies thus formed are compensated by both gaseous oxygen and bulk lattice oxygen. The turning point at  $x = 0.9$ , for both the electrical conductivity and the activity, was associated with the oxygen occupancy of different lattice sites in the YBCO crystal. Generally, Ovenston and Walls have found the a.c. techniques to be more reliable and informative when ions and electronic charge carriers are present at high temperatures [50].

The total conductivity is likely to be highly sensitive to the processing and pre-history of a sample and to whether it has been subjected to thermal cycling above about 773 K or to rapid cooling [23, 25]. Such factors must be taken into account when considering the potential for YBCO as a catalyst to be heated by r.f. power. There are many other mixed oxides of high electrical conductivity which may also have potential for use at radio frequencies, and some of these are currently being studied. Factors involved in the chemical synthesis of advanced ceramic powders have recently been summarized by Luss, [51] Sleight [52] and Segal [53]. The lack of thermodynamic stability in these materials is a predominant issue, although perovskites are generally thermally and chemically very stable and some have the necessary electrical properties [54]. The various routes towards optimal synthesis should be considered in future work.

In a recent review on ion and mixed conducting oxides as catalysts, Gellings and Bouwmeester [55] concluded that the conducting properties of these oxidic materials exert a great influence on their catalytic behaviour; only a limited number of systematic investigations have been performed on the correlation between the catalytic and conduction properties. This ongoing research should help fill the gaps. In a catalytic reaction, the surface properties are of prime importance; thus there is an urgent need to study the relations between the surface and bulk conduction properties. The a.c. techniques, newly applied to catalytic composites [36] should help elucidate such relationships.

## 5. Conclusion

The oxygen-deficient, high-temperature superconductor  $\text{YBa}_2\text{Cu}_3\text{O}_{7-x}$  has been shown to act as a catalyst for the oxidation of methane. In a conventional tubular reactor fed with methane and operating at 1000 K, the production of CO and  $\text{CO}_2$  is accompanied by a decrease in activity and a reduction in conductivity as

lattice oxygen in the catalyst is used up. The activity and conductivity return to their initial states after re-oxidation of the catalyst in air. Thus the reaction may be monitored by following changes in the conductivity of the catalyst under *in-situ* conditions.

This material, when mixed with 50 wt % alumina has been shown to have ideal electrical characteristics for absorbing energy from a reactor operating at 20 MHz. Temperatures up to 1000 K may be rapidly attained and maintained without the problems of thermal runaway sometimes encountered with other mixed-oxide conductors, which have a high activation energy for the conductivity near reaction temperatures.

At radio-frequencies, preliminary experiments have shown that the reaction products contained some ethylene and ethane in addition to total oxidation products. Further work on a larger-scale reactor should clarify the efficacy of this technique for the partial oxidation of methane and other oxidation reactions. The facile removal or replacement of lattice oxygen is known to be beneficial for the partial-oxidation reaction, thus this route offers considerable potential when coupled with the rapid control of temperature possible with the electromagnetic heating technique.

## Acknowledgements

The authors gratefully acknowledge the provision of equipment with grants from the SERC.

## References

1. A. OVENSTON, S. MIRI and J. R. WALLS *Brit. Ceram. Soc. Proc.* **43** (1988) 57.
2. A. OVENSTON and J. R. WALLS, *Trans. I. Ch. E.* **68** (1990) 530.
3. A. W. SLEIGHT, *Science* **208** (1980) 895.
4. J. M. THOMAS, *Adv. Mater.* **8** (1989) 255.
5. M. T. MIRZA, J. R. WALLS and S. A. A. JAYAWEERA, *Thermochimica Acta* **152** (1989) 203.
6. J. R. WALLS, J. K. LEE and A. OVENSTON in Proceedings of the Eight International Symposium on Chemical Reactor Engineering, Edinburgh, 10–13 Sept., 1984. **87** Edited by G. S. G. Beveridge and P. N. Rowe. (Inst. Chem. Engrs., Rugby 1984) 463.
7. N. D. PARKYNS, *Chem. Brit.* **26** (1990) 841.
8. M. G. POIRIER, A. R. SANGER and K. J. SMITH, *Can. J. Chem. Engng.* **69** (1991) 1027.
9. S. MIRI, PhD thesis. University of Teesside, Middlesbrough 1993.
10. J. M. THOMAS, *Solid State Ionics* **32–33** (1989) 869.
11. J. J. CARBERRY, S. RAJADURAI, C. B. ALCOCK and B. LI, *Catal. Lett* **4** (1990) 43.
12. S. RAJADURAI, J. J. CARBERRY, B. LI and C. B. ALCOCK, *J. Catal.* **131** (1991) 582.
13. I. J. PICKERING and J. M. THOMAS, *J. Chem. Soc. Faraday Trans.* **87** (1991) 3067.
14. J. C. OTAMIRI and S. L. T. ANDERSSON, *Appl. Catal.* **73** (1991) 267.
15. I. HALASZ, A. BRENNER, M. SHELEF and K. Y. S. NG, *J. Catal.* **126** (1990) 109.
16. S. HANSEN, J. C. OTAMIRI and A. ANDERSSON, *Catal. Lett.* **6** (1990) 33.
17. A. T. ASHCROFT, A. K. CHEETHAM, M. L. H. GREEN, L. P. GREY and P. D. F. VERNON, *J. Chem. Soc. Chem. Commun.* **21** (1989) 1667.

18. A. T. ASHCROFT, A. K. CHEETHAM, J. S. FOORD, M. L. H. GREEN, C. P. GREY, A. J. MURRELL and P. D. H. VERNON, *Nature* **344** (1990) 319.
19. J. H. WHITE, E. A. NEEDHAM, R. L. COOK and F. SAMMELLS, *Solid State Ionics* **53-56** (1992) 149.
20. B. C. H. STEELE, I. KELLY, H. MIDDLETON and R. RUDKIN, *ibid.* **28-30** (1988) 1547.
21. S. SEIMANIDES, P. TSIKARAS, X. E. VERYKIOS and C. G. VAYENAS, *Appl. Catal.* **68** (1991) 41.
22. J.-L. DUBOIS and C. J. CAMERON, *ibid.* **67** (1990) 49.
23. J. NOWOTNY, M. REKAS and W. WEPPNER, *J. Amer. Ceram. Soc.* **73** (1990) 1040.
24. N. P. BANSAL, *J. Mater. Res.* **3** (1988) 1304.
25. W. CARRILLO-CABRERA, H. D. WIEMHOFER and W. GÖPEL, *Solid-State Ionics* **32-33** (1989) 1172.
26. A. BELZNER, T. M. GÜR and R. A. HUGGINS, *ibid.* **40-41** (1990) 535.
27. H. L. TULLER and E. OPILA, *ibid.* **40-41** (1990) 790.
28. J. NOWOTNY and M. REKAS, *J. Amer. Ceram. Soc.* **73** (1990) 1048.
29. *Ibem.*, *ibid.* **73** (1990) 1054.
30. J. MOLEND, A. STOKLOSA and T. BAK, *Physica C* **175** (1991) 555.
31. F. MUNAKATA, K. SHINOHARA, H. KANESAKA, N. HIROSAKI, A. OKADA and M. YAMANAKA, *Jpn. J. Appl. Phys.* **26** (1987) L1292.
32. J. X. ZHANG, G. M. LIN, W. G. ZENG, K. F. LIANG, Z. C. LIN, G. G. SIU, M. J. STOKES and P. C. W. FUNG, *Supercond. Sci. Technol.* **3** (1990) 163.
33. T. MATSUI, T. FUJITA, K. NAITO and T. TAKESHITA, *J. Solid State Chem.* **88** (1990) 579.
34. G. DELL'AGLI, O. MARINO, P. MASCOLO, A. DI CHARA, G. PEPE and U. SCOTTO DI UCCIO, *J. Mater. Sci. Mater. in Elec.* **1** (1990) 20.
35. T. KOMATSU, O. TANAKA, C. HIROSA, K. MATSUTA and T. YAMASHITA, *J. Mater. Sci. Lett.* **9** (1990) 170.
36. A. OVENSTON and J. R. WALLS, *Solid State Ionics* **53-56** (1992) 825.
37. J. R. MACDONALD "Impedance spectroscopy" (Wiley, New York, 1987).
38. R. ANDORF and M. BAERNS, *Catal. Today* **6** (1990) 445.
39. J. H. EDWARDS, K. T. DO and R. J. TYLER, *Stud. Surf. Catal.* **61** (1991) 489.
40. D. W. LEYSHON, *ibid.* **61** (1991) 497.
41. F. M. DAUTZENBERG, J. C. SCHLATTER, J. M. FOX, J. R. ROSTRUP NIELSEN and L. J. CHRISTIANSEN, *Catal. Today* **13** (1992) 503.
42. J. H. LUNSFORD, *ibid.* **6** (1990) 235.
43. *Idem.* *Stud. Surf. Catal.* **61** (1991) 3.
44. H. SHIMADA, S. MIYAMA, and H. KURODA, *Chem. Lett.* **110** (1988) 275.
45. H. YOKOKAWA, N. SAKAI, T. KAWADA and M. DOKIYA, *Solid State Ionics* **40-41** (1990) 398.
46. H. YOKOKAWA, T. KAWADA and M. DOKIYA, *J. Amer. Ceram. Soc.* **72** (1989) 2104.
47. A. OVENSTON and J. R. WALLS, *Solid State Ionics* **44** (1991) 251.
48. R. SPINICCI, *Stud. Surf. Catal.* **61** (1991) 173.
49. A. JIANG, Y. PENG, Q. W. ZHOU, P. Y. GAO, H. Q. YUAN and J. F. DENG, *Catal. Lett.* **3** (1989) 235.
50. A. OVENSTON and J. R. WALLS, *J. Catal.* **140** (1993) 464.
51. D. LUSS, *Chem. Engng. Sci.* **45** (1990) 1979.
52. A. W. SLEIGHT, *Phys. Today* **44** (1991) 24.
53. D. SEGAL "Chemical synthesis of advanced ceramic materials" (Cambridge University Press, Cambridge, 1989).
54. V. J. M. VERMEIREN, I. D. M. L. LENOTTE, J. A. MARTENS and P. A. JACOBS, *Stud. Surf. Catal.* **61** (1991) 33.
55. P. J. GELLINGS and H. J. M. BOUWMEESTER, *Catal. Today* **12** (1992) 1.

*Received 31 March  
and accepted 26 August 1993*